IEEE Access
Multidisciplinary | Rapid Review | Open Access Journal

Received March 30, 2020, accepted April 19, 2020, date of publication April 30, 2020, date of current version May 15, 2020.

Digital Object Identifier 10.1109/ACCESS.2020.2991658

Achieving High UAV Uplink Throughput by Using Beamforming on Board

TOMASZ IZYDORCZYK[1], GILBERTO BERARDINELLI[1], PREBEN MOGENSEN[1,2], MICHEL MASSANET GINARD[1], JEROEN WIGARD[2], AND ISTVÁN Z. KOVÁCS[2]

[1]Wireless Communication Networks Section, Department of Electronic Systems, Aalborg University, 9220 Aalborg, Denmark
[2]Nokia Bell Labs, 9220 Aalborg, Denmark

Corresponding author: Tomasz Izydorczyk (ti@es.aau.dk)

ABSTRACT High-throughput unmanned aerial vehicle (UAV) communication may unleash the true potential of novel applications for aerial vehicles but also represents a threat for cellular networks due to the high levels of generated interference. In this article, we investigate how a beamforming system installed on board a UAV can be efficiently used to ensure high-throughput uplink UAV communications with minimum impact on the services provided to users on the ground. We study two potential benefits of beamforming, namely, spatial filtering of interference and load balancing, considering different beam switching methodologies. Our analysis is based on system-level simulations followed by a series of measurement campaigns in live Long-Term Evolution (LTE) networks. Our results show that using UAV-side beamforming has a great potential to increase uplink throughput of a UAV while mitigating interference. When beamforming is used, even up to twice as many UAVs may be served within a network compared with UAVs using omni-directional antennas, assuming a constant uplink throughput target. However, to fully exploit the potential of beamforming, a standardized solution ensuring alignment between network operators and UAV manufacturers is required.

INDEX TERMS Aerial vehicles, beamforming, cellular network, interference management, LTE, UAV, uplink.

I. INTRODUCTION

Unmanned aerial vehicle (UAV) communications have shown potential to enable a plethora of new services, such as delivery of goods or infrastructure inspection [1]. Reliable and ubiquitous command and control (C2) connectivity everywhere in the air is required to support beyond visual line of sight flights [2]. The C2 link itself may however not be sufficient to satisfy some demanding use cases as surveillance or real-time video broadcasting UAVs. In such scenarios, a minimum guaranteed uplink bit rate of 10 Mbps is required to satisfy the demands of transmitting video frames in high definition to the cloud servers [3], [4].

Cellular networks have been recognized as the most promising wireless technology to serve UAVs [5]. Due to their almost everywhere deployment, as well as favorable signal propagation characteristics at lower frequency bands, cellular networks have been shown to be capable of meeting the requirements imposed by the C2 communication link [6].

The associate editor coordinating the review of this manuscript and approving it for publication was Mauro Fadda.

However, due to increased line of sight (LoS) probability of the air to ground (A2G) channel, uplink streaming UAVs may create immense uplink interference toward multiple base stations (BSs), impacting their observed uplink signal-to-interference-plus-noise ratio (SINR) [7]. This impact is expected to be even more severe when the predicted number of UAVs flying simultaneously over the same region (e.g., city) grows, harming not only the selfish uplink demands of other UAVs but negatively impacting the coexistence with ground user equipments (GdUEs), as presented in Figure 1.

Different techniques aiming at coping with increased interference levels and providing UAV connectivity have been proposed in the literature. Massive multiple input multiple output (MIMO) with 3D beamforming capabilities assumed at the BSs is proposed among others in [8], [9] and [10]. By pointing the beams toward the flying UAVs, the potential communication link can be strengthened, while other links may observe reduced interference as the beams are pointed in different directions. Interference coordination among multiple cells is proposed in [11]. The work in [12] further extends the concept of interference mitigation and investigates the

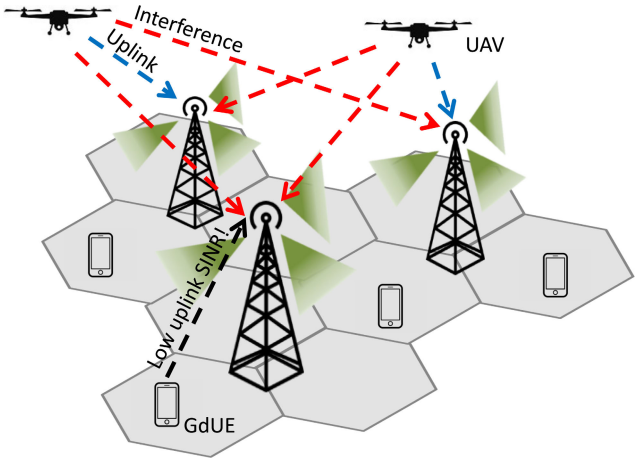

FIGURE 1. Impact of uplink interference created by flying UAVs.

possible UAV assistance in the process. The 3rd Generation Partnership Project (3GPP) within the Release 15 studies on UAV enhancements for Long-Term Evolution (LTE) [13] proposes among others a UAV-specific power control settings such that highly interfering UAVs can be issued to lower their transmit power and therefore reduce the interference.

Although all of the mentioned solutions show the potential of serving a future flying UAV, they may require hardware changes at the network side. This, especially in the early deployment phase, when only a limited number of UAVs are expected, may be costly and not profitable. Furthermore, even when the number of flying UAVs increases, UAVs should be able to fly anytime and anywhere, demanding large investments in the cellular networks.

Implementing a beamforming system on board UAVs is recognized as an alternative solution in [14] and [15]. The authors show the effects of the directional antenna pattern on observed interference and SINR levels, indicating the potential benefits of this solution. They also indicate that it is much cheaper to invest in UAVs, and it may allow them to fly anywhere. However, both works are limited only to the performance of the C2 link, without considering high uplink throughput communication.

In this work, the potential of UAV-side beamforming to satisfy high uplink throughput demands of UAVs is thoroughly investigated using both system-level simulations and experimental measurements over live cellular networks. The main focus is to show how beamforming can be used to spatially filter the radiated interference and in effect improve the uplink performance of UAVs while ensuring fair coexistence with GdUEs. Additionally, the potential of beam steering for load balancing is studied, showing how a UAV's uplink throughput can be improved by steering the beam toward the directions of less interfered/loaded cells. To achieve this goal, a Reference Signal Received Quality (RSRQ)-based beam switching algorithm is proposed and compared with conventional Reference Signal Received Power (RSRP)-based beam switching. Finally, both presented concepts are validated during a series of measurement campaigns using a real UAV with a set of directional antennas and connectivity to live LTE networks.

The rest of this paper is structured as follows. In Section II, the expected benefits of using beamforming are explained followed by a presentation of two studied beam switching algorithms. Further, in Sections III and IV, the system-level simulation settings and results are presented, respectively. Section V presents the results of the measurement campaign, further validating the performance of UAV-side beamforming. Discussion and recommendations reflecting on the obtained results are provided in Section VI. The work is concluded in Section VII.

II. THE BENEFITS OF BEAMFORMING ON BOARD A UAV

A beamforming system installed on a UAV can bring many potential benefits stemming from not only antenna gain but also directionality. These benefits can be grouped into two categories: spatial filtering of interference and load balancing due to beam steering. Both are further described below, focusing on uplink (UAV to BS) communication link.

- **Spatial filtering of interference:** Due to high LoS probability, a transmitted signal from a UAV will be received by many cells, effectively reducing their uplink SINR and thus leading to decreased uplink throughput of their users. The problem becomes more severe if there are multiple UAVs flying over the same region. Their uplink interference will accumulate leading to even worse overall system performance in the affected cells.
  Using beamforming and focusing the signal toward the direction of a serving cell, a UAV can minimize the amount of radiated energy toward other BSs located outside of the main antenna beam. This principle is known as spatial filtering of interference [16]. By spatially filtering the interference, only a limited number of cells, coinciding with the direction of the main beam will be interfered. Limiting interference will lead to higher uplink SINR levels observed in the network and thus improved uplink throughput for the users in these cells - both GdUEs and UAVs.
- **Spatial load balancing:** Any user of the cellular network may experience connection to high and low loaded cells, which lead to different achievable throughput. Flying UAVs will require a constant, high uplink throughput to meet the demands of some use-cases. However, UAVs, as all other users in the network, can be attached to a high loaded cell, which is not able to meet UAV communication requirements.
  By using beamforming on board a UAV, the freedom of choosing the beamforming direction can be used for spatial load balancing. By steering the beam away from a loaded cell, a UAV's uplink throughput can potentially be improved as the network may perform a handover to a different cell. Although load balancing is practically available in the network even without beamforming [17], it requires cooperation between multiple cells to know

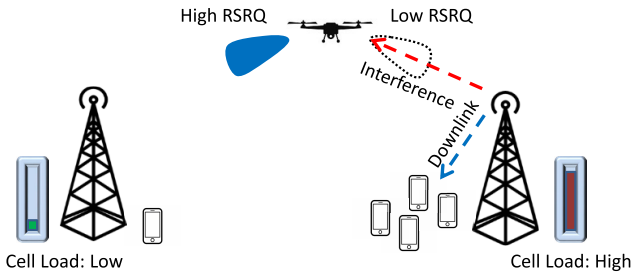

FIGURE 2. The principle of using RSRQ-based beam switching for load balancing.

their instantaneous load. In this article, we demonstrate how beamforming together with RSRQ-based beam switching can be used to achieve load balancing without the cooperation requirements imposed on cellular networks.

A. STUDIED UAV BEAM SWITCHING ALGORITHMS

In this article, two UAV beam switching algorithms are studied. First, the RSRP-based beam switching method is used. In this case, a flying UAV instantaneously selects the beam resulting in the highest RSRP, providing a handover threshold Δ_{A3} is satisfied [18]. Such beam selection ensures the cell with the strongest received signal power is used.

To showcase load balancing properties, RSRQ-based beam switching is also implemented. In this case, a UAV chooses the beam based on the highest RSRQ, which is defined as the ratio between the measured RSRP and the total received power including desired and interfering signals [19]. Figure 2 explains how the RSRQ metric captures the effects of network load and can be used for load balancing purposes. As presented in the figure, a flying UAV is located in the proximity of a high loaded cell, which does not have sufficient available resources to meet the UAV's uplink demands. When the loaded cell is serving its ground users, the flying UAV receives these downlink transmissions as interference, effectively reducing the measured RSRQ toward this direction. However, when the UAV is pointing its beam toward a more distant but less loaded cell, even though the distance to the cell is larger, the amount of observed interference is limited, resulting in a higher RSRQ; therefore, a connect to the less loaded cell is made.

III. SYSTEM-LEVEL SIMULATION SETTINGS

In the first part of this article, system-level simulations are used to show the potential impact of beamforming in multi-UAV scenarios. A dynamic system-level simulator thoroughly described in [14] is used. To best show the practical aspects of the proposed results, a real network topology of a Danish network operator was implemented in the simulator, with real locations, heights, antenna patterns and orientations of more than 150 cells representing the city of Aalborg and its suburbs. Contrary to the work in [14] focusing on a rural network and sub-GHz frequency bands, in this article, the implemented network represents a system deployed at a 1.8 GHz carrier frequency and 20 MHz bandwidth.

TABLE 1. Parameters used in system-level simulations.

Parameter	Value
Simulation area	40x40 km
Network layout	Real imported network layout
Number of cells	162
System bandwidth	20 MHz
Carrier frequency	1800 MHz
Total number of GdUEs	Scenario dependent, 750 or 1200
UAV's flying height	40 m
GdUE's height	1.5 m
UAV's velocity	Scenario dependent, 30 km/h or hovering
GdUE's velocity	Pedestrian speed (5km/h)
UAV's channel model	Height-dependent model [20]
GdUE's channel model	Urban Macro
Uplink traffic	Full buffer model
Max uplink transmit power	23 dBm
Uplink power control P_0	-58 dBm per PRB (180 kHz)
Uplink power control α	0.75
Handover event	A3 with Δ_{A3}=3 dB
Number of iterations	100
Length of one iteration	20 s

A height-dependent UAV channel model derived in [20] is used in the simulator. The channel model used for GdUEs is the urban macro model from 3GPP specifications [21]. Further, we consider open-loop power control. The algorithm can be described as follows:

$$P_{UL} = \min\{P_{UL}^{max}, P_0 + \alpha RSRP_{est} + 10\log_{10} M\}, \quad (1)$$

where P_{UL} and P_{UL}^{max} represents the used and maximum allowed uplink transmit powers, respectively. $RSRP_{est}$ and M represent the estimated RSRP and number of scheduled uplink resource blocks. Finally, P_0 and α are two network controlled parameters, which are adjusted in this simulation with respect to the imported network layout such that most of the users can transmit with lower power than P_{UL}^{max}. Table 1 summarizes the most relevant settings of the simulator.

Flying UAVs are equipped with six directional antennas and a switching system, as described in [14] and presented in Figure 3. Each of the six antennas points toward a different direction and has a beamwidth of 60°. All antennas have 6.6 dBi directional gain and −13 dB front-to-sidelobe ratio. The antenna system orientation is fixed with respect to the fuselage.

A. CONSIDERED SCENARIOS

To show the benefits of beamforming, three different scenarios are studied, as summarized in Table 2. First, Scenario 1 focuses on the potential of beamforming for spatial filtering of interference. A low-loaded network is designed with a target of two average active GdUEs per cell moving with pedestrian speed. Different numbers of flying UAVs are dropped within the simulated area. UAVs fly at 30 km/h in a random direction at 40 m height. This setup emulates the envisioned package delivery scenario and represents last-mile delivery service.

TABLE 2. Scenarios studied using system-level simulations.

Scenario	Research target	Possible use-case	Number of UAVs	GdUEs distribution	UAV distribution
Scenario 1	Spatial filtering of interference	Last-mile package delivery	1 - 100 UAVs	Low load (Average 2 active users per cell), random movement at 5 km/h	UAVs drawn uniformly, random flight patterns at 30 km/h
Scenario 2	Load balancing	An event with real-time TV broadcasting	1 - 5 UAVs	Low load (Average 2 active users per cell, random movement at 5 km/h) plus a crowded region (50 GdUEs drawn in a 100 m^2 square corresponding to average 17 active users per cell, static)	UAVs drawn randomly over a crowded region, hovering
Scenario 3	Joint effect of spatial filtering and load balancing	A UAV flying in a highly populated area during rush hour	1 - 100 UAVs	Medium load (Average 3.5 users per cell, random movement at 5 km/h) and five crowded regions (50 GdUEs drawn in a 100 m^2 square corresponding to average 17 active users per cell, static) distributed across the map	UAVs drawn uniformly, random flight patterns at 30 km/h

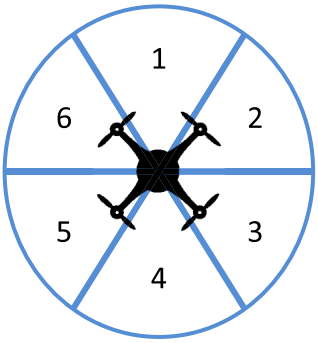

FIGURE 3. Modeled antenna beam configuration of a UAV.

Scenario 2 focuses on showcasing the spatially controlled load balancing using beamforming. For this reason, a 'crowd' of static 50 GdUEs is generated in the 100 m$\times$100 m central, most urban region with a limited number of UAVs drawn at 40 m height hovering right above the crowd. The remaining GdUEs are drawn uniformly within a network, considering low load as in Scenario 1. This scenario emulates any event in which many users are located in a certain place and flying UAVs are used to either monitor or for real-time broadcasting of video footage.

Finally, in Scenario 3, the focus is placed on the worst case scenario in which a loaded network is generated. In addition, five randomly placed crowded events, as described in the previous scenario, are drawn and are happening simultaneously. UAVs are drawn randomly within the frame of the city and behave as in Scenario 1.

Two different beam switching algorithms are used in all three scenarios as explained in Section II. For comparison, in all three scenarios, the case of UAVs using omnidirectional antennas is also studied. Each scenario is repeated 100 times. In each iteration, UAVs and GdUEs are randomly repositioned and move with the assigned scenario-dependent velocity for 20 s.

B. MEASUREMENT KPIs

To understand the impact of beamforming on the performance of UAVs and GdUEs, the following key performance indicators (KPIs) are considered:

- **UAV-originated uplink interference over thermal noise (IoT):** The overall uplink interference quantified per cell, normalized such that 0 dB represents the average IoT when no UAVs (only GdUEs) are available in the network.
- **Uplink SINR:** Average uplink SINR of users with active uplink transmissions. Studied separately for UAVs and GdUEs.
- **Uplink throughput:** Average uplink throughput. Studied separately for UAVs and GdUEs. Because the main objective of this work being to study the performance of beamforming to meet high uplink throughput demands of UAVs, a 10 Mbps target is used in some analysis. This represents the minimum requirements for real-time video streaming.

IV. SIMULATION RESULTS

A. SCENARIO 1 - SPATIAL FILTERING OF INTERFERENCE

First, the focus is on spatial filtering of uplink interference using beamforming as described in Section II and labeled as Scenario 1. Figure 4a presents the average levels of UAV-originated uplink IoT averaged over different cells. With more flying UAVs, the overall IoT values increase as more uplink transmissions are made. Spatial filtering of interference becomes visible when a larger number of UAVs is simultaneously flying, with more than 4 dB reduction of interference power for the case of 100 UAVs. Both beam

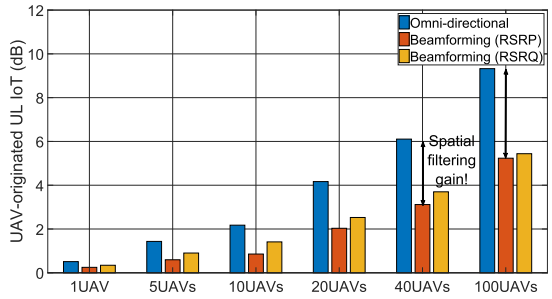

(a) Rise of UAV-originated uplink Interference observed by the cells

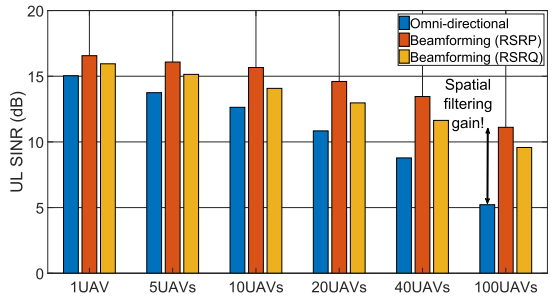

(b) Uplink SINR of flying UAVs

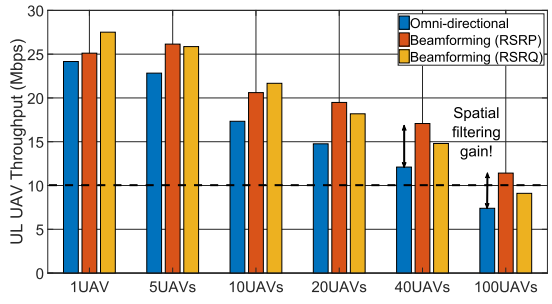

(c) Average uplink throughput of flying UAVs

FIGURE 4. Simulation results of Scenario 1.

switching algorithms result in a similar IoT increase. The slightly lower average IoT levels in the case of RSRP-based beam switching are a result of the uplink power control algorithm, as in Equation (1), where path loss is estimated based on $RSRP_{est}$. RSRP-based switching always selects the beam with the best RSRP, leading to the lowest uplink transmit power and therefore lowest radiated interference.

Second, in Figure 4b, the uplink SINR values averaged over all flying UAVs are shown. The impact of spatial filtering can be seen. The results are clearly correlated with the IoT results discussed earlier. With a larger number of UAVs, increased interference leads to reduced SINR values with a more than 5 dB SINR drop for 100 UAVs.

Finally, the impact of interference and reduced SINR on uplink throughput of the UAVs can be seen in Figure 4c. The overall throughput values drop with more UAVs in the network. Spatial filtering of interference impacts the observed throughput values, leading to improved performance. Some interesting observations can be made. With only a single flying UAV, uplink throughput observed with an omni-directional antenna and using RSRP-based beam switching

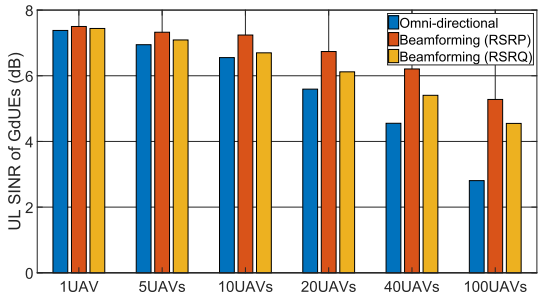

FIGURE 5. Average uplink SINR of ground users.

is almost identical and is consistent with the measurement results presented in [22]. This is because, with only a single UAV, spatial filtering of interference is not yet visible as there are no other interfering UAVs to affect the performance. In addition, uplink power control compensates the antenna gain leading to the same average uplink throughput.

Given a low-loaded network, even with 40 UAVs, the benchmark 10 Mbps uplink throughput, marked using the dashed line, is exceeded regardless of the antenna system. However, with more UAVs, only using beamforming, the target value can be achieved. Finally, this figure also indicates that about two times more UAVs can be supported in the network when beamforming is used compared to omni-directional UAVs assuming the same uplink throughput target.

A fair coexistence between flying UAVs and GdUEs is necessary for smooth adoption of UAVs into the cellular paradigm. To showcase how beamforming impacts the performance of ground users, Figure 5 presents the average uplink SINR of all GdUEs. Similarly to Figure 4b, the SINR values drop with more UAVs. However, due to spatial filtering of interference, the drop is reduced if UAVs use beamforming. The improved uplink SINR can be translated into better overall uplink throughput ensuring improved performance of GdUEs in the presence of UAVs.

B. SCENARIO 2 - IMPACT OF SPATIALLY CONTROLLED LOAD BALANCING DURING A CROWDED EVENT

The potential of using beamforming for load balancing while flying over a crowded event is discussed in this subsection. Figure 6 presents the observed values of uplink SINR and uplink throughput for 1, 2 and 5 flying UAVs. By studying only a limited number of UAVs, the effect of load balancing can be isolated from the spatial filtering effect discussed previously. The SINR values for both beamforming strategies are similar regardless of the number of UAVs. However, the uplink throughput in the case of RSRQ-based beamforming is twice the throughput when RSRP-based beam switching is used. This indicates the potential of using RSRQ as a beam switching metric to improve load balancing properties.

Note that the overall SINR and throughput of UAVs are still relatively low, even when RSRQ-based beam switching is used. This can be explained as follows. When a UAV is able to connect to a relatively low loaded cell, such cell is

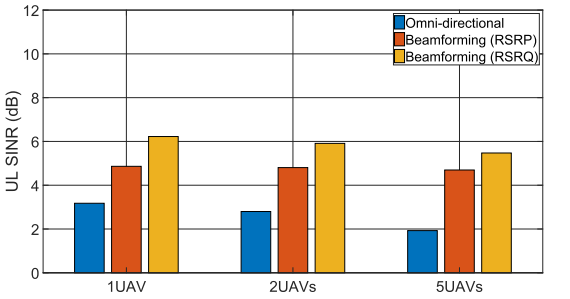

(a) Uplink SINR when UAVs fly in loaded cell

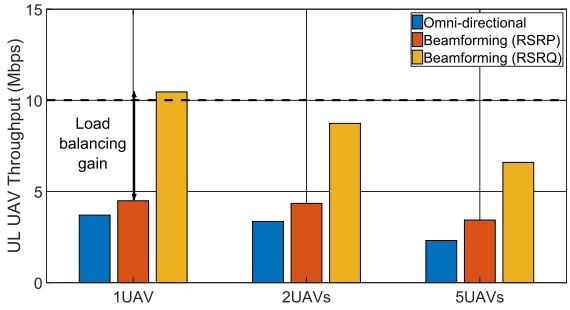

(b) Uplink throughput when UAVs fly in loaded cell

FIGURE 6. Simulation results of Scenario 2.

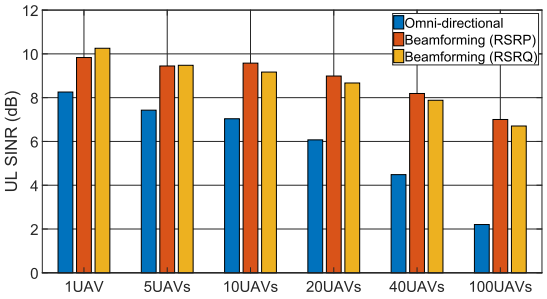

(a) Uplink SINR of flying UAVs in a loaded network

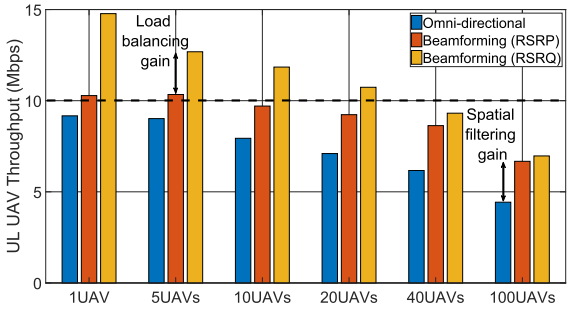

(b) Average uplink throughput of flying UAVs in a loaded network

FIGURE 7. Simulation results of Scenario 3.

still likely to be one of the closest physically located cells. In such a case, all the GdUEs located in a crowd are still causing a significant uplink interference to the UAV's serving cell, limiting its SINR and the UAV's uplink throughput.

The impact of spatially controlled load balancing on the GdUE's performance is rather limited with respect to the already studied spatial filtering and therefore not shown in the paper. If a UAV is connected to the same cell, it competes for an already limited set of resources with GdUEs, limiting their potential uplink throughput. If a UAV is connected to a low loaded cell located in close proximity, it acts as an interferer to the cell serving GdUEs, effectively reducing their uplink SINR.

C. SCENARIO 3 - PERFORMANCE OF SPATIAL FILTERING AND LOAD BALANCING IN A LOADED NETWORK

Finally, the potential of beamforming is studied in the presence of a loaded network with multiple events happening in different places. As in Scenario 2, Figure 7 presents the average uplink SINR and throughput for different numbers of flying UAVs. Both spatial filtering of interference and load balancing effects are visible when analyzing the uplink throughput results. Not surprisingly, spatial filtering gains are dominant when a larger number of UAVs is flying and interfering the network.

Load balancing gains are a major reason for throughput improvement with a limited number of UAVs, when interference-based load balancing can still be used to connect to a low loaded cell. The load balancing gains disappear however with a very high number of UAVs and result in similar uplink throughput to the one obtained using RSRP-based beam switching as fewer and fewer cells remain low-loaded and interfered.

To obtain the target 10 Mbps uplink throughput, an RSRQ-based beamforming strategy is to be used even with a limited number of UAVs. The overall network load is indeed too high to achieve the target when omni-directional antennas or RSRP-based beamforming is used.

V. EXPERIMENTAL MEASUREMENT CAMPAIGNS

After disclosing the potential of uplink beamforming using system-level simulations, a set of measurement campaigns was conducted to experimentally validate the spatial filtering of interference and load balancing properties of beamforming as well as to analyze UAV-GdUEs coexistence.

The measurements were conducted using the platform presented in [22], consisting of a UAV with six directional antennas, one omni-directional antenna and an LTE modem, as presented in Figure 8. The antennas used in the measurement system are virtually identical with the model used in the previously described simulations. Both measurement campaigns were conducted using a real LTE network deployed at 1.8 GHz with UAVs flying over the same region (and network) as implemented in the system-level simulator and presented in Figure 9.

Due to practical restrictions, this initial measurement campaign was conducted using only a single flying UAV. Nevertheless, as argued in Section IV, even a single flying UAV is sufficient to experimentally validate the presence of spatial filtering or load balancing.

A. VALIDATION OF SPATIAL FILTERING OF INTERFERENCE

The first measurement campaign focused on validating in practice the spatial filtering of interference. The goal of this study is to compare the uplink IoT levels observed within a network in the case that a UAV is using omni-directional

transmission or beamforming. To achieve this goal, two thirty-minute flights were performed in Aalborg, Denmark, in which a UAV hovering at 100 m constantly executed a full-buffer uplink transmission. During the first flight, the UAV used the omni-directional antenna, while during the second flight, transmission was beamformed toward a predefined direction. The IoT information was obtained based on network IoT KPI data provided by the network operator. The measurements were taken during nighttime hours, in which the overall non-UAV interference in the network is negligible.

To validate the spatial filtering, the average interference increase Δ_{IoT} is computed in dB as follows:

$$\Delta_{\text{IoT}} = \text{IoT}_{\text{Omni}} - \text{IoT}_{\text{Beamforming}} - \text{IoT}_{\text{No UAVs}}. \quad (2)$$

Figure 9 presents the obtained Δ_{IoT} values per cell across the network. The UAV position together with the antenna patterns are presented. The obtained results are visualized using a color code, in which green colors represent cells where the omni-directional antenna created higher levels of interference than the directional antenna ($\Delta_{\text{IoT}} > 0$dB); red colors represent cells which where interfered more using the directional antenna ($\Delta_{\text{IoT}} < 0$dB). The darker the colors are, the larger the difference.

The obtained results give visual indication that omni-directional transmission creates more spatially spread interference than beamforming. In some cells, omni-directional transmission create more than 7 dB higher interference than the beamforming system. Only a limited number of cells observe higher interference when beamforming is used. However, even in these cases the increase in interference is limited and does not exceed 2 dB.

In Figure 10, similar results obtained using different beamforming directions are presented. The results are presented in terms of total IoT per cell located at a relative angle with respect to the flying UAV. When a UAV uses an omni-directional antenna, cells located in every direction are being interfered. However, when using beamforming, only cells located within the main beam observe interference higher than 4 dB. Moreover, within the main beam direction, the interference levels observed for the very same cells when using both antenna systems are comparable. Due to uplink power control, beamforming can therefore spatially filter interference without increasing it in the direction of the main beam.

Finally, the average IoT when there are no UAV transmissions is presented to further indicate that when measuring during nighttime hours, most of the interference observed in the network is initiated by a flying UAV, and the impact of GdUE-originated interference can be omitted from the analysis.

B. VALIDATION OF LOAD BALANCING

The target of the second measurement campaign was to showcase the potential of using beamforming for load balancing while ensuring the coexistence between UAVs and GdUEs. Similar to Scenario 2 of the simulations, measurements

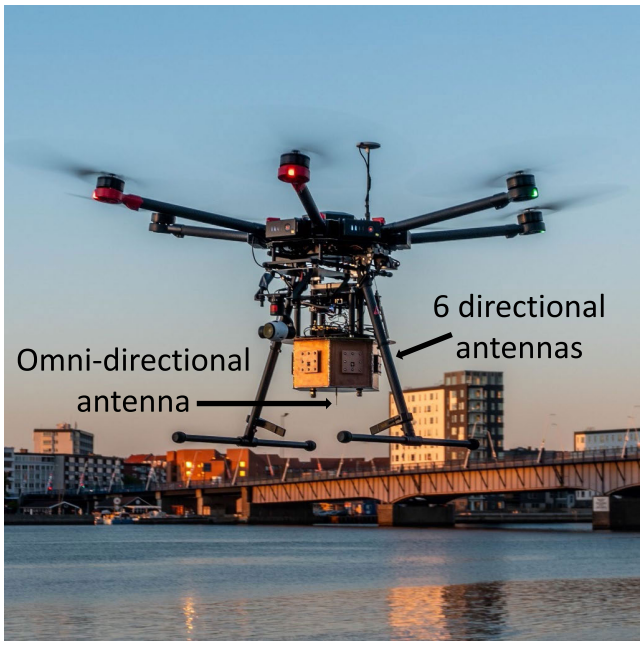

FIGURE 8. Active UAV during one of the measurement campaigns.

were used to show the possibility of triggering a network handover when switching the beamforming direction, thus escaping a loaded cell to improve UAV uplink throughput. Four Release 13-compatible, Cat. 18 mobile phones [23], with installed Qualipoc [24] software to measure network parameters were used as GdUEs. They were all located in the same place and connected to the same cell. All phones were programmed for a full buffer uplink transmission such that a loaded cell was created (referred to later as *cell A*). A UAV was set to hover at 40 m right above the GdUEs, also performing a full-buffer uplink transmission.

For the first 15 minutes, the flying UAV was using an omni-directional antenna and based on the recorded logs, it attached to the same cell as the GdUEs (cell A). Further, for the next 15 minutes, the UAV was programmed to use the directional antenna pointing in the opposite direction of the location of cell A. Eventually, the change in the antenna system triggered a handover procedure to a different cell (referred to later as *cell B*).

This beam switching,[1] although simplified, resembles the RSRQ-based beam switching, as studied in the simulation phase. By pointing the beam away from cell A, a network handover toward cell B was triggered. The conducted measurements reflect similar conditions as in Scenario 2 from the system-level simulations; as in both cases, a UAV flew directly over a group of GdUEs.

Figure 11 presents the empirical cumulative distribution function (ECDF) of recorded UAV uplink throughput during the measurements, while in Figure 12, the ECDF of the GdUE uplink throughput is presented. It is clearly visible that both types of devices benefit from load balancing. Initially, the

[1]Please refer to [22] for details of how the switching was implemented.

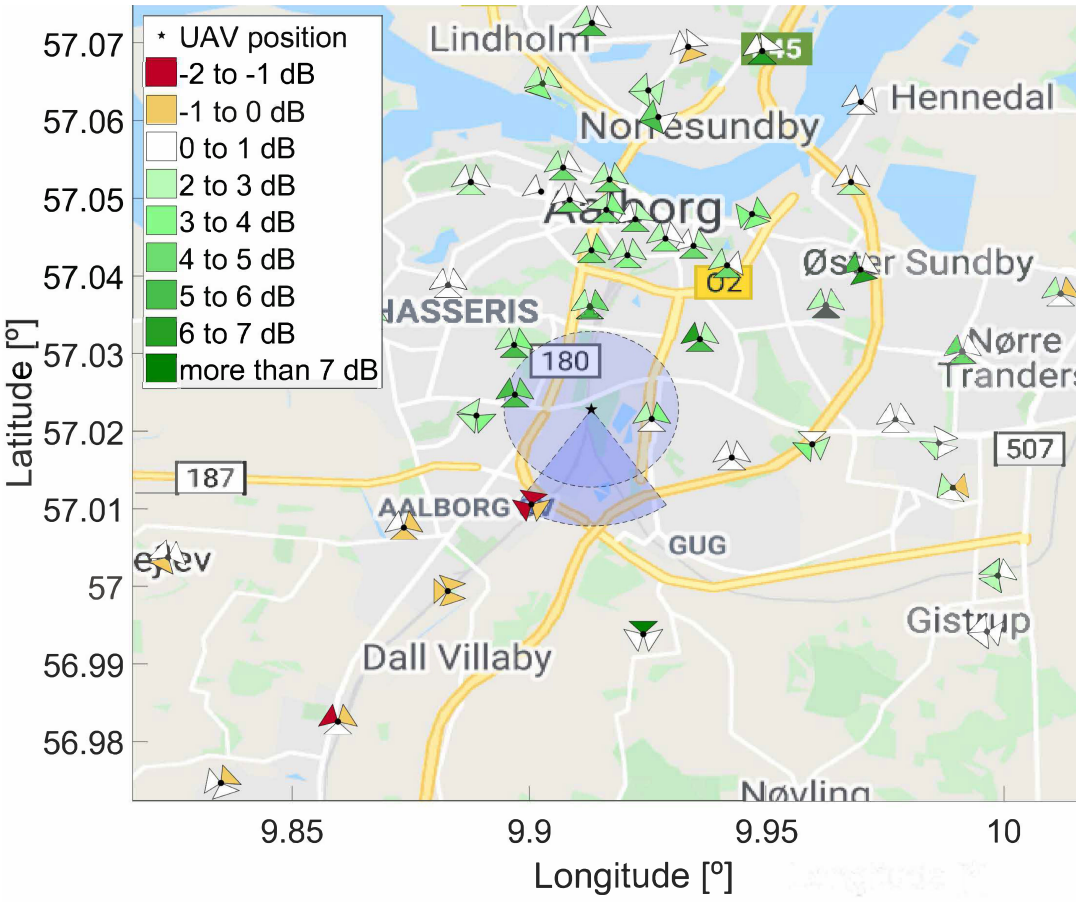

FIGURE 9. Map of Aalborg, presenting the uplink Δ_{IoT} observed at different cells.

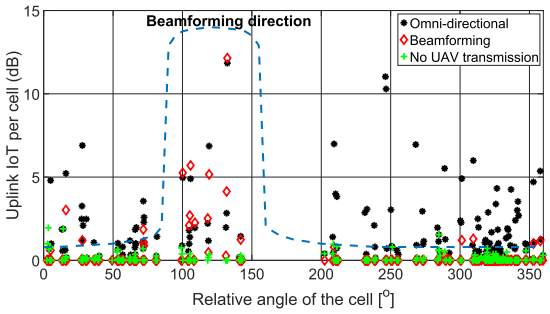

FIGURE 10. Experimentally observed spatial interference mitigation when using beamforming.

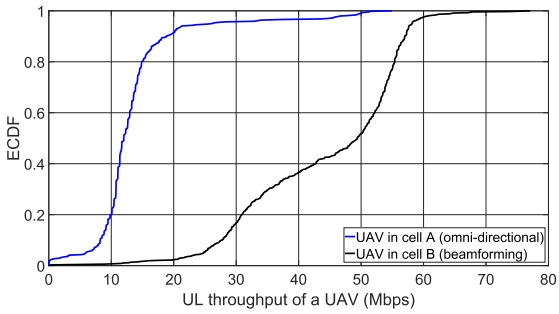

FIGURE 11. Uplink throughput of the UAV during load balancing experiments.

UAV observes low uplink throughput because it was connected to a loaded cell A. The median throughput of the UAV increases approximately five times after handover to cell B is performed.

Similar behavior is observed regarding uplink throughput of GdUEs. The low throughput due to a large number of active devices (4 GdUEs and 1 UAV) increases by more than 12% when the UAV switches cell and frees the resources. Theoretically, the throughput should increase by 25%. The lower gain is due to the interference generated by the UAV to cell A. Figure 13 presents the ECDF of uplink transmit power for all GdUEs. There is more than a 10 dB increase in the average transmit power when the UAV transitions from being a user of the same cell to an interferer (handover from cell A to cell B).

Although the actual power control policy implemented in a real network is unknown, the obtained results indicate that the UAV uplink transmission to cell B resulted in strong interference to cell A, and all GdUEs in cell A were set to a higher uplink transmit power to compensate otherwise decreased uplink SINR. We believe that the real network is using an SINR estimate to make fast adjustments of the UE uplink transmit power on top of the usual open-loop power control based on $RSRP_{est}$. However, in the performed simulations,

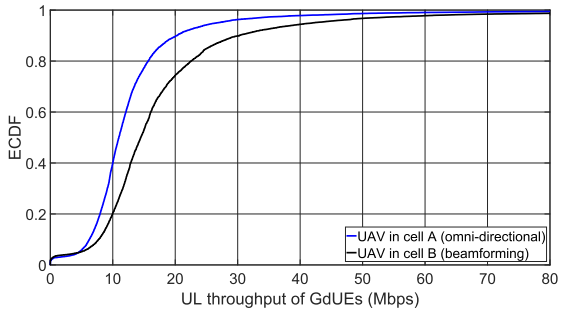

FIGURE 12. Uplink throughput of the GdUEs during load balancing experiments.

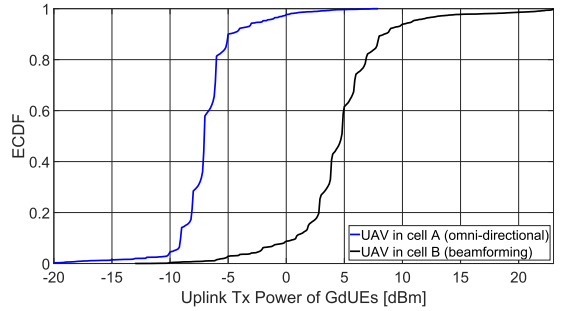

FIGURE 13. Uplink transmit power of the GdUEs during load balancing experiments.

these fast adjustments were not implemented. Nonetheless, our obtained experimental results are aligned with the results reported by other researchers in [25].

VI. DISCUSSION AND RECOMMENDATIONS

In the remainder of this article, we summarize our findings, discuss their impact and provide some guidelines on the potential future improvements needed for seamless integration of UAVs within a cellular network. The experimental results provided in Section V validated the concepts studied using system-level simulations presented in Section IV. In the authors' opinion, they provide valuable information on how today's network can handle UAV traffic and show that there is still a lot to be done to meet all UAV requirements within a cellular network framework.

UAV-side beamforming has shown a great potential to mitigate uplink interference by spatially directing the uplink transmission only in a desired direction. This behavior leads to improved uplink throughput of flying UAVs and ensure fair coexistence with GdUEs. Bearing in mind that there are multiple network-side interference mitigation techniques already in use or proposed, UAV-side beamforming should be regarded as a complementary technique, further used to reduce interference. The promises of beamforming are also clearly visible when a UAV is flying in a high traffic cell. In this situation, beamforming can be used to steer the connectivity and potentially improve UAV uplink throughput with limited interference impact on the nearby cells.

A. UAV-CONTROLLED BEAMFORMING

In the simulations and during the described experiments, a mobile network (simulated or real-world) did not possess any knowledge of flying UAVs and their beamforming capabilities.[2] In such a situation, it is up to the UAV to choose the desired beamforming direction. During the simulations, beam switching was performed considering RSRP or RSRQ metrics. During the measurements, due to limitations of the used modem, the executed beamforming direction was chosen manually based on the analysis of network topology.

Leaving the beamforming decision to the UAV itself, although already providing visible gains, is clearly suboptimal from both UAV and mobile network operator perspectives. A UAV, even if a smart beamforming algorithm is implemented, would have to assume the beamforming direction without any guarantees that it is beneficiary. As an example, during the measurement campaign validating load balancing, the UAV might direct the beam toward a cell that is even more loaded, or even worse, in the direction where there are no cells at all. Although eventually a UAV may find a correct beamforming direction (by performing trial and error beam sweeps), while sweeping, the uplink throughput requirements of a UAV may not be satisfied.

When the beamforming decision is taken by the UAV, the potential spatial interference reduction gains are also suboptimal. Assuming a multi-UAV scenario, it may happen that each UAV chooses its beamforming direction independently in such a way that the interference radiating from all UAVs will accumulate in a certain geographical region. In the worst case, the highly interfered region, would observe similar interference as if all UAVs are equipped with an omni-directional antennas.

B. NETWORK-ASSISTED BEAMFORMING

To fully embrace the potential of beamforming on the UAVs, a network needs to not only possess the knowledge but also be in control of beamforming decisions of each UAV. If the network has the capabilities to signal the beamforming direction to each UAV present within a certain geographical area, highly optimized interference and load balancing procedures can be used. If multiple UAVs are present, an optimized network would be able to redirect their beams over base stations located at directions for which mutual harm is avoided.

A load balancing procedure would become beneficial if a UAV demands constant high uplink throughput. Due to the larger amount of visible cells by a UAV, the network would be able to proactively redirect a UAV to a cell in which the trade-off between low cell load and potential impact on GdUEs is satisfied. By doing so, the demands of the UAV can be satisfied and coexistence with GdUEs improved.[3] One example can be a UAV flying over a city center and being connected to a cell located in the suburban or residential area with a lower load.

[2]While performing the measurements, we used a regular SIM card with a commercial data plan

[3]Contrary to the performed measurements in Section V-B, where using UAV-controlled beamforming, UAV demands were satisfied with the risk of increasing intercell interference.

Network assistance will also become beneficial during crowded events. In Scenario 2 of the simulations presented in Section IV-B, due to high uplink IoT, a UAV flying over a crowd of users observed limited uplink throughput, not matching the minimum 10 Mbps target. It is expected that with network assistance, a handover to a cell with low IoT can be made and the minimum throughput target can be achieved.

C. UAV-SPECIFIC UPLINK POWER CONTROL

Another way that the network can benefit from UAV-sided beamforming is by introducing a UAV-specific uplink power control. Please note that as of Release 15, a UE-specific power control is already available and can be used to differentiate the uplink power assignments for the particular group of users [26]. Considering UAVs with beamforming capabilities as one of such groups, a network can create unique power control settings embracing directional gains.

Assuming a power control policy in which a group of UAVs with beamforming capabilities can transmit their uplink signals with higher power compared with regular power control settings, stronger signals will be received by the serving cell allowing higher-order modulation to be used at a UAV and therefore improving uplink throughput. This gain comes at the expense of increased interference radiated within the main beam of the UAV. However, this extra interference can be in some situations tolerated by the network if the beam direction is carefully controlled and steered in the potentially less loaded directions.

VII. CONCLUSION

High-throughput uplink UAV communication is a necessary technology component needed to fully benefit from UAVs flying in our skies. In high load scenarios or with many UAVs flying over the same geographical region, cellular networks may not be able to match these stringent requirements. By implementing a beamforming system on a UAV, its efficient usage may complement network efforts in providing high uplink throughput for UAVs. In this article, we have analyzed potential scenarios in which such a beamforming system would become beneficiary. As a result of the conducted simulations and experiments, we indicated the limitations of the current generation of cellular networks and provided possible guidelines on how to efficiently integrate high uplink-demanding UAVs into the cellular paradigm.

ACKNOWLEDGMENT

The authors would like to thank TDC, Denmark, for supporting this work by sharing the network topology and the IoT information.

REFERENCES

[1] Y. Zeng, Q. Wu, and R. Zhang, "Accessing from the sky: A tutorial on UAV communications for 5G and beyond," *Proc. IEEE*, vol. 107, no. 12, pp. 2327–2375, Dec. 2019.

[2] S. Hayat, E. Yanmaz, and R. Muzaffar, "Survey on unmanned aerial vehicle networks for civil applications: A communications viewpoint," *IEEE Commun. Surveys Tuts.*, vol. 18, no. 4, pp. 2624–2661, 2016.

[3] P. Chandhar and E. G. Larsson, "Massive MIMO for connectivity with drones: Case studies and future directions," *IEEE Access*, vol. 7, pp. 94676–94691, 2019.

[4] S. Qazi, A. S. Siddiqui, and A. I. Wagan, "UAV based real time video surveillance over 4G LTE," in *Proc. Int. Conf. Open Source Syst. Technol. (ICOSST)*, Dec. 2015, pp. 141–145.

[5] X. Lin, V. Yajnanarayana, S. D. Muruganathan, S. Gao, H. Asplund, H.-L. Maattanen, M. Bergstrom, S. Euler, and Y.-P.-E. Wang, "The sky is not the limit: LTE for unmanned aerial vehicles," *IEEE Commun. Mag.*, vol. 56, no. 4, pp. 204–210, Apr. 2018.

[6] *LTE Unmanned Aircraft Systems Trial Report*, Qualcomm, San Diego, CA, USA, May 2017.

[7] R. Amorim, H. Nguyen, J. Wigard, I. Z. Kovacs, T. B. Sorensen, D. Z. Biro, M. Sorensen, and P. Mogensen, "Measured uplink interference caused by aerial vehicles in LTE cellular networks," *IEEE Wireless Commun. Lett.*, vol. 7, no. 6, pp. 958–961, Dec. 2018.

[8] A. Garcia-Rodriguez, G. Geraci, D. Lopez-Perez, L. G. Giordano, M. Ding, and E. Bjornson, "The essential guide to realizing 5G-connected UAVs with massive MIMO," *IEEE Commun. Mag.*, vol. 57, no. 12, pp. 84–90, Dec. 2019.

[9] Y. Zeng, J. Lyu, and R. Zhang, "Cellular-connected UAV: Potential, challenges, and promising technologies," *IEEE Wireless Commun.*, vol. 26, no. 1, pp. 120–127, Feb. 2019.

[10] G. Geraci, A. Garcia-Rodriguez, L. Galati Giordano, D. Lopez-Perez, and E. Bjornson, "Understanding UAV cellular communications: From existing networks to massive MIMO," *IEEE Access*, vol. 6, pp. 67853–67865, 2018.

[11] W. Mei, Q. Wu, and R. Zhang, "Cellular-connected UAV: Uplink association, power control and interference coordination," *IEEE Trans. Wireless Commun.*, vol. 18, no. 11, pp. 5380–5393, Nov. 2019.

[12] W. Mei and R. Zhang, "UAV-sensing-assisted cellular interference coordination: A cognitive radio approach," *IEEE Wireless Commun. Lett.*, early access, Jan. 30, 2020, doi: 10.1109/LWC.2020.2970416.

[13] *Summary for WI Enhanced LTE Support for Aerial Vehicles*, document RP-181644, 3GPP, Sep. 2018.

[14] H. C. Nguyen, R. Amorim, J. Wigard, I. Z. Kovacs, T. B. Sorensen, and P. E. Mogensen, "How to ensure reliable connectivity for aerial vehicles over cellular networks," *IEEE Access*, vol. 6, pp. 12304–12317, 2018.

[15] T. Izydorczyk, M. Bucur, F. M. L. Tavares, G. Berardinelli, and P. Mogensen, "Experimental evaluation of multi-antenna receivers for UAV communication in live LTE networks," in *Proc. IEEE Globecom Workshops (GC Wkshps)*, Dec. 2018, pp. 1–6.

[16] B. D. Van Veen and K. M. Buckley, "Beamforming: A versatile approach to spatial filtering," *IEEE ASSP Mag.*, vol. 5, no. 2, pp. 4–24, Apr. 1988.

[17] H. Hu, J. Zhang, X. Zheng, Y. Yang, and P. Wu, "Self-configuration and self-optimization for LTE networks," *IEEE Commun. Mag.*, vol. 48, no. 2, pp. 94–100, Feb. 2010.

[18] *LTE Evolved Universal Terrestrial Radio Access (E-UTRA). Radio Resource Control (RRC). Protocol Specification*, document TS 36.331 Version 15.3.0, 3GPP, Oct. 2018.

[19] *LTE Evolved Universal Terrestrial Radio Access (E-UTRA). Physical Layer. Measurements*, document TS 36.214 Version 14.2.0, 3GPP, Apr. 2017.

[20] R. Amorim, H. Nguyen, P. Mogensen, I. Z. Kovacs, J. Wigard, and T. B. Sorensen, "Radio channel modeling for UAV communication over cellular networks," *IEEE Wireless Commun. Lett.*, vol. 6, no. 4, pp. 514–517, Aug. 2017.

[21] *Spatial Channel Model For Multiple Input Multiple Output (MIMO) Simulations*, document TR 25.996, 3GPP, Mar. 2011.

[22] T. Izydorczyk, M. Massanet Ginard, S. Svendsen, G. Berardinelli, and P. Mogensen, "Experimental evaluation of beamforming on UAVs in cellular systems," 2020, *arXiv:2003.12010*. [Online]. Available: http://arxiv.org/abs/2003.12010

[23] *LTE Evolved Universal Terrestrial Radio Access (E-UTRA). User Equipment (UE) Radio Access Capabilities*, document TS 36.306 Version 14.2.0, 3GPP, Apr. 2017.

[24] *Using R&S TSMA With Swiss Qual Qualipoc Android. A Wide Range of Optimization Applications*, Rohde and Schwarz, Munich, Germany2016.

[25] J. Sae, R. Wiren, J. Kauppi, H.-L. Maattanen, J. Torsner, and M. Valkama, "Public LTE network measurements with drones in rural environment," in *Proc. IEEE 89th Veh. Technol. Conf. (VTC-Spring)*, Apr. 2019, pp. 1–5.

[26] C. Ubeda Castellanos, D. L. Villa, C. Rosa, K. I. Pedersen, F. D. Calabrese, P.-H. Michaelsen, and J. Michel, "Performance of uplink fractional power control in UTRAN LTE," in *Proc. VTC Spring*, May 2008, pp. 2517–2521.

TOMASZ IZYDORCZYK received the M.Sc. degree in mobile communications from Télécom ParisTech/Eurecom, in 2017. He is currently pursuing the Ph.D. degree with Aalborg University (AAU). In 2016, he was a Research Intern with Intel Mobile Communications, Sophia Antipolis, France. His research interests include MIMO techniques for V2X and UAV communications, focusing on their experimental verification.

GILBERTO BERARDINELLI received the bachelor's and master's degrees *(cum laude)* in telecommunication engineering from the University of L'Aquila, Italy, in 2003 and 2005, respectively, and the Ph.D. degree from Aalborg University, Denmark, in 2010. He is currently an Associate Professor with the Wireless Communication Networks (WCN) section, Aalborg University, and works in tight cooperation with Nokia Bell Labs. He is an author or coauthor of more than 100 international publications, including conference proceedings, journal contributions, and book chapters. His research interests are mostly focused on physical layer, medium access control, and radio resource management design for 5G systems.

PREBEN MOGENSEN received the M.Sc. and Ph.D. degrees from Aalborg University, in 1988 and 1996, respectively. Since 1995, he has been a part-time Associate with Nokia. Since 2000, he has been a Full Professor with Aalborg University, where he is currently leading the Wireless Communication Networks section. He is also a Principal Scientist with Nokia Bell Labs and a Nokia Bell Labs Fellow. He has coauthored over 400 articles in various domains of wireless communication. His Google Scholar H-index is 61. His current research interests include the 5G industrial IoT and technology components towards 6G.

MICHEL MASSANET GINARD received the B.Sc. degree in telecommunication engineering from the Technical University of Madrid, in 2018. He is currently pursuing the M.Sc. degree in wireless communication systems with Aalborg University (AAU). He has participated in UAV experimental studies as a Student Research Assistant. His current research interests are related to cellular network performance and emerging technologies for 5G wireless networks.

JEROEN WIGARD received the M.Sc. degree in electrical engineering from Technische Universiteit Delft, Netherlands, in 1995, and the Ph.D. degree on the topic of handover algorithms and frequency planning in frequency hopping GSM networks from Aalborg University, Denmark, in 1999. He joined Nokia Aalborg, Denmark, where he worked on radio resource management-related topics for 2G, 3G, 4G, and 5G networks. He is currently with Nokia Denmark Bell Labs, Aalborg (former Nokia Networks Aalborg) and is involved in studies and 5G standardization related to UAVs and nonterrestrial networks (NTN). He has authored and coauthored over 60 journals and conference papers and holds more than 80 patent applications.

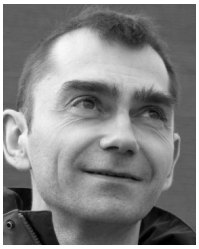

ISTVÁN Z. KOVÁCS received the B.Sc. degree from the Politehnica Technical University of Timişoara, Romania, in 1989, the M.Sc.E.E. degree from the École Nationale Supérieure des Télécommunications de Bretagne, France, in 1996, and the Ph.D.E.E. degree in wireless communications from Aalborg University, Denmark, in 2002. He is currently a Senior Research Engineer with Nokia Bell Labs, Aalborg, Denmark, where he conducts research on machine learning-driven RRM and radio connectivity evolution for nonterrestrial and aerial vehicle communications in LTE and 5G networks.